Effect of chitosan-coated and pure PLLA scaffolds composition and structure on the chondrogenesis of mesenchymal stem cells

Joana Magalhães, PhD,[1,2] Myriam Lebourg, PhD,[1,3], Harmony Deplaine, PhD,[3] José Luis Gómez Ribelles, PhD,[1,3] Francisco J. Blanco, MD, PhD[2]

[1] Biomedical Research Networking Center in Bioengineering, Biomaterials and Nanomedicine (CIBER-BBN), Spain.

[2]Grupo de Bioingeniería Tisular y Terapia Celular (CBTTC-CHUAC). Servicio de Reumatología. Instituto de Investigación Biomédica de A Coruña (INIBIC). Complexo Hospitalario Universitario de A Coruña (CHUAC). Sergas. Universidade da Coruña (UDC). As Xubias, 15006. A Coruña, Spain.

[3]Centro de Biomateriales e Ingeniería Tisular, Universidad Politécnica de Valencia. Camino de Vera s/n 46071, Edificio 8E, Planta 1. Valencia, Spain.

Correspondence should be sent to: Francisco J. Blanco, Joana Magalhães. Grupo de Bioingeniería Tisular y Terapia Celular (CBTTC-CHUAC). Servicio de Reumatología. Instituto de Investigación Biomédica de A Coruña (INIBIC). Complexo Hospitalario Universitario de A Coruña (CHUAC). Sergas. Universidade da Coruña (UDC). As Xubias, 15006. A Coruña, Spain. Tel: +34981176399. Fax: +34981176398 Email: fblagar@sergas.es, joana.cristina.silva.magalhaes@sergas.es

Abstract

Due to the attractive properties of poly(L-lactic acid) (PLLA) and chitosan (CHT) for tissue engineering applications, this study is aimed at analyzing the chondrogenic potential of human bone marrow derived-mesenchymal stem cells (BM-MSCs) in PLLA, pure or combined with CHT, using different coating methodologies. Whilst PLLA scaffolds coated in one-step (PLLA-CHT1) yielded CHT smooth pellicles within PLLA macropores, a two-step strategy resulted in a CHT fiber-like coating within PLLA micropores. Both strategies led to the incorporation of similar content of CHT and a 2-fold increase in the scaffolds water uptake capacity, providing elastic moduli values comparable to the ones found for human articular cartilage. After confirming BM-MSCs metabolic activity in PLLA-CHT scaffolds, the chondrogenic potential was tested at 30 and 60 days, in a chondrogenic differentiation medium. PLLA scaffolds improved the chondrogenic differentiation of BM-MSCs, regarding cell pellet conventional culture. On the long term, pure PLLA induced the production of a transient cartilage-like phenotype that couldn't be reverted by the presence of chitosan. Moreover, the process of CHT coating led to differences on the MSCs chondrogenic differentiation process, forming either rather heterogeneous tissues, with confined areas of faster maturation or slower cell infiltration (PLLA-CHT1), or a more homogeneously distributed extracellular matrix (PLLA-CHT2), which could be useful for developing a zonal distribution typically presented in healthy articular cartilage.

Keywords: mesenchymal stem cells, poly(L-lactic acid), chitosan, cartilage tissue engineering, osteoarthritis

1. INTRODUCTION

Osteoarthritis (OA) is a degenerative disease characterized by the degradation of articular cartilage. (1) One of the primary risk factors for OA is joint injury, and cartilage defects, such as focal chondral or osteochondral lesions, tend to progress in people with symptomatic OA. (2) Human bone marrow mesenchymal stem cells (BM-MSCs) have been presented as candidate cells for cartilage repair due to their ability to undergo chondrogenic differentiation after extensive expansion *in vitro* and stimulation with various biomaterials. (3, 4)

The nature and physicochemical properties of three-dimensional scaffolds offer opportunities for lineage-specific biochemical and biophysical cues to enhance selective differentiation of MSCs and subsequent production of matrix. (5-7) Hybrid scaffolds are therefore attractive to create biomimetic environments promoting the formation of complex tissues such as those found in the osteochondral milieu. To date, a range of biomaterial scaffolds based on natural and synthetic origin polymers have been widely investigated for tissue repair and regeneration. (8-10)

Poly(L-lactic acid) (PLLA) is a commonly used synthetic polymer that can be fabricated into complex shapes via a wide range of technologies presenting tunable mechanical and structural properties. (11, 12) This FDA-regulated material is biocompatible, and degrades gradually to natural metabolites, having been used clinically in both bone and cartilage repair strategies. (13, 14)

However, due to PLLA inherent hydrophobic nature, different studies have pointed out the reduction of expression of osteoblastic phenotypic markers as well as a negative influence on cell attachment and proliferation, due to the

denaturation of adhesive ligands of cells. (13) In order to overcome these drawbacks, several groups have focused on the grafting of hydrophilic and/or natural origin materials to PLLA, improving tissue repair and regeneration processes. (15-19) Chitosan (CHT), [poly-β(1-4)-2-amino-2-deoxy-D-glucose], is one of the most abundant natural amino polysaccharides, with structural characteristics similar to glycosaminoglycans (GAGs) present in the extracellular matrix of cartilage. It is known to be non-toxic, biocompatible and biodegradable. (20, 21) Moreover, the presence of $-NH_2$ groups, makes it soluble in acid solutions. (22) The applications of cationic chitosan include drug delivery, growth factor encapsulation and gene delivery. (23, 24)

In this work, PLLA scaffolds were modified using CHT following two different coating strategies. We investigated the influence of their morphology and chemical composition on the chondrogenic differentiation of BM-MSCs, providing more insight for their potential as scaffolds for osteochondral tissue engineering applications.

2. Materials and methods

2.1. Materials

2.1.1. PLLA scaffold fabrication

PLLA scaffolds were prepared by a mixed technique of phase separation and porogen as described previously. (25, 26) Shortly, PLLA (Cargill Dow) solution in dioxane (15% w/v) was mixed to an equal quantity of acrylic microspheres (Lucite International) in a Teflon crystallizer and quenched in liquid nitrogen. Dioxane extraction was carried out by ethanol washes, at -20 ºC, for three days followed by porogen extraction using ethanol, at 40 ºC, until the acrylic filler was

no longer detected in the washing solvent. Scaffolds were air-dried during 24h and afterwards under vacuum until constant weight.

2.1.2. PLLA-CHT scaffold fabrication

PLLA scaffolds were filled with a chitosan solution (0.5% w/v, Novamatrix) in acetic acid (1%), under vacuum. For PLLA-CHT1, excess CHT was removed and scaffolds were quenched in liquid nitrogen; for PLLA-CHT2, CHT coating was dried at 37 ºC for 24h; this procedure was repeated three times. Then chitosan filling or coating was gelled at -20 ºC, in a pre-cooled sodium hydroxide (0.1M)-ethanol solution (1:1), during 3 days. (27, 28) Subsequently, samples were extensively washed in distilled water, until pH remained neutral, and either: freeze-dried (PLLA-CHT1) under 0.001 mbar for 48h (Lyoquest, Telstar), or air-dried for 24h and thereafter under vacuum (PLLA-CHT2) until constant weight.

2.2. Characterization

2.2.1. Morphology

Prior observation with scanning electron microscopy (SEM), samples were cryofractured in liquid nitrogen and mounted on copper stubs with graphite adhesive tape. Samples were gold sputtered and observed in a JEOL JSM6300 microscope, at an acceleration tension of 15kV.

2.2.2. Porosity

Porosity was determined by a gravimetric method, as the quotient of the volume of pores and the total volume of the scaffold. Briefly, dry samples were weighed, filled with ethanol under vacuum, and re-weighed. The volume of pores, V_{pore}, was obtained from the weight difference between the dry (m_{dry}) and wet (m_{wet}) sample, according to equation (1) assuming that the amount of ethanol

absorbed by the blends is negligible, during the time of the experiment. Thus, the volume of the pores equals the volume occupied by the absorbed ethanol.

$$V_{pore} = \frac{m_{wet} - m_{dry}}{d_{ethanol}} \quad (1)$$

where $d_{ethanol}$ is the density of ethanol. The volume occupied by the polymer was calculated from the dry weight of the scaffold assuming a density of PLLA of 1.29 g/cm^3 for crystalline phase and 1.19 g/cm^3 for amorphous phase. (29)

Five measurements were carried out for each scaffold.

2.2.3. Chitosan content in PLLA-CHT samples

Thermogravimetric analysis (SDTQ600, TA Instruments) was used to determine the quantity of CHT effectively coated. The samples (triplicate) were subjected to a temperature ramp from room temperature until 800 ºC, at 20 ºC/min under nitrogen flow (50 ml/min). The quantity of CHT in the samples was determined based on the fact that CHT leaves a dry residue of 30% at 700 ºC whilst PLLA does not leave any.

2.2.4. Equilibrium swelling ratio

For water content analysis, samples (n = 5) were immersed in distilled water, until equilibrium was reached (48h). Samples were weighed in the dry (Wd) and wet (Ws) states and the equilibrium swelling ratio was calculated according to equation (2):

$$\text{Equilibrium Swelling Ratio} = \frac{Ws}{Wd} \quad (2)$$

2.2.5. Unconfined compression tests

Samples were submitted to a compression ramp in a Microtest standard compression machine with a 15N load cell. For wet samples, scaffolds were hydrated with distilled water, at room temperature, for 24h. Using the

methodology from ASTM D1621-04a norm "Compression of rigid cellular plastics", for compression testing of porous samples, modulus (E) was calculated from a linear regression of the elastic zone and the yield strength (Ys), that represents the value of tension by which the pores start to collapse, was determined as the stress value at the end of the elastic zone and beginning of the plateau zone. Five measurements were performed.

2.3. Cells

Human mesenchymal stem cells were isolated from bone marrow (BM) samples obtained from seven patients undergoing total hip replacement due to osteoarthritis. All patients signed an informed consent agreement form, approved by the Ethics Committee of Clinical Research of Galicia (CEIC). BM-MSCs were cultured in expansion medium (EM) composed by Dulbecco's modified Eagles medium (DMEM) supplemented with 20% fetal bovine serum (FBS) and penicillin/streptomycin (10,000 IU/mL) (all from Sigma-Aldrich) until 90% confluent. Pre-plating technique was performed in order to avoid any remaining fibroblasts. (3) Phenotypic characterization and multipotential characterization (adipogenic and osteogenic differentiation) were performed using standardized protocols. (30)

2.4. Cellular studies

2.4.1. Viability Assay

PLLA, PLLA-CHT1 and -CHT2 scaffolds (6mm Ø x1mm) were sterilized prior to cell seeding. Briefly, 3 x 10^5 BM-MSCs (P3), suspended in 50 µl EM were seeded on the scaffolds (each in triplicate) placed individually on a 24-well cell culture plate and allowed to adhere for 2h before the addition of 1 ml of EM. Cellular metabolic activity was followed during 48h, 14 and 30 days, using the

alamar blue manufacturer's specifications (Invitrogen). Cells-only cultured on tissue-cultured polystyrene wells (TCPS) were used as reference.

2.4.2. Chondrogenic differentiation

BM-MSCs were seeded in pure and CHT-coated PLLA, as previously described, and incubated in a well-defined chondrogenic differentiation medium (CM) composed by DMEM supplemented with knock-out serum (15%), ascorbic acid (10 µl/ml), transferrin (6 µl/ml), dexamethasone (10 µM), retinoic acid (10^{-7} M) and transforming growth factor beta 3 (TGF-β3, 10 ng/ml), at 37 ºC, under 5% CO_2, for 30 and 60 days. MSC pellet culture system was modified from Zhang *et al.*, and used as control. (31) Briefly, 2.5 x 10^5 cells, suspended in 500 µl CM, were centrifuged at 600 x g for 10 min, in 15-ml polypropylene conical tubes. Pelleted cells were incubated in the same conditions as cell-constructs.

2.4.3. Histology and immunohistochemistry

Pellets from BM-MSCs, following differentiation into chondrocyte-like cells, were frozen in OCT embedding matrix (Sakura). Bisected cell-constructs were fixed in 4% (w/v) paraformaldehyde (Sigma) and embedded in paraffin. Histological staining was performed with hematoxylin and eosin (HE), safranin-O (SaO), toluidine blue (TB), as well as alizarin red and Von Kossa staining, in order to detect matrix mineralization. Immunohistochemical labeling was performed for collagen type-II (col-II), aggrecan and lubricin; collagen type- I (col-I) and type-X (col-X). For this, cryosections of 4 µm were deparaffinised, hydrated in serial graded alcohol, pre-treated with chondroitinase-ABC (Sigma) and immunostained with monoclonal antibodies. Secondary antibodies were detected using a polymer-labelled HRP complex (Kit Envision Detection Systems Peroxidase/DAB, DAKO) with diaminobenzidine substrate.

Quantification of positive expression for collagens was performed using analiSIS software (version D) (Olympus). The values were expressed as the percentage of positive staining normalized against the total area of matrix produced.

2.4.4. Gene expression analysis

Total RNA was isolated from both cell-pellets and cell-constructs using a RNeasy minikit (Quiagen). Briefly, samples were transferred to RNase-free microcentrifuge tubes containing cell lysis buffer from the RNeasy minikit and pulverized in a micro-dismembrator (Retsch MM200). Complete homogenization was performed using a QIAshredder column. The homogenates were then transferred to spincolumns from the RNAeasy minikit according to the manufacturer's protocol. The RNA samples were treated with DNase and converted into cDNA using the SuperScript VILO cDNA synthesis kit (Invitrogen). Gene expression was measured by real-time reverse transcription polymerase chain reaction (qRT-PCR), conducted in a LightCycler® 480 Instrument (Roche) using the LightCycler® 480 Probes Master protocol. Amplification of mRNA was performed using custom primers shown in Table 1. Beta-2-Microglobulin (B2M) and Ribosomal Protein L13a (RPL13a) were used as housekeeping genes (HKG). Relative levels of expression were calculated by the $2^{-\Delta\Delta Ct}$ method. (32) Data were normalized against the values obtained for the cell-pellet control for each gene, which was assigned the value of 1, and were measured as relative expression levels.

2.5. Statistical analysis

All data presented are expressed as mean ± standard deviation (SD). Statistical comparisons were carried out using one-way analysis of variance (ANOVA). Values of $p < 0.05$ were considered statistically significant.

3. Results

3.1. Morphology and porosity

Freeze-gelation, extraction and drying processes were critical in influencing scaffolds architecture, depicted in Figure 1. PLLA scaffolds present a double porosity (macro and micro), spherical interconnected pores (153±51µm) and a porosity of 88±2% (Figure 1A). The steps involved in CHT coating, did not seem to affect the microporous structure of PLLA but mainly how CHT coating remained distributed within the scaffold. On one hand in PLLA-CHT1, the hydrogel phase of CHT filled the macroporous space of the PLLA scaffold, as rather continuous smooth pellicles (arrow on Figure 1B). On the other hand in PLLA-CHT2 (Figure 1C), CHT tended to generate a fibrous-like coating over PLLA micropores. Nonetheless, PLLA-CHT2 overall porous structure was found very similar to pure PLLA.

3.2. CHT content and equilibrium swelling ratio

The decomposition profiles for PLLA, PLLA-CHT1 and -CHT2 are represented in Figure 2A. On a first region of thermal degradation, up to 200 ºC, the weight loss differences among the pure and coated PLLA are linked to the presence of moisture due to the introduction of the hydrophilic component - CHT. For both CHT-coated PLLA, the onset of PLLA thermal degradation shifted to lower temperatures, which is correlated to a slight decrease observed for the molecular weight (S01). After the main degradation, chitosan was obtained as the final product, with 5±0.8% (PLLA-CHT1) and 6±1% (PLLA-CHT2) contents.

Incorporation of CHT into hydrophobic PLLA scaffolds provoked an increase of the swelling ratio which was found similar, 8.3±0.5 (PLLA-CHT1) and 8.3±0.7 (PLLA-CHT2), despite of the coating methodology followed (Figure 2B).

3.3. Mechanical properties

Strain stress curves are represented in **Error! Reference source not found.** 3 (A, B). These can be divided in three zones as usually observed in porous scaffolds; (33) The first linear zone corresponds to the elastic deformation of the whole structure (strain 0-0.15); a second linear zone, with reduced slope corresponds to the progressive bending of the struts between the pores, according to the material porosity (strain 0.15-0.5), which leads to a structure densification with increasing slope (strain 0.5-0.8). Whereas only the first zone is observed in pure PLLA, in both CHT-coated PLLA scaffolds one can observe the three aforementioned zones. The strain-stress profiles show a similar trend in both dry (Figure 3A) and wet states (Figure 3B), even though the slopes are generally reduced in the latest due to the loss of rigidity in the presence of water. As observed in Figure 3 (C, D), PLLA shows major rigidity and strength, in both states, with minor variation related to its hydrophobicity. CHT-coating induced a softening of pure PLLA (2.28±0.45 MPa), expressed by a decrease of the modulus value; 0.82±0.1 MPa and 0.73±0.36 MPa for PLLA-CHT1 and -CHT2, respectively, in the dry state (Figure 3C). In concurrence, the yield strength (Figure 3D) follows the same trend, revealing decreased values of 0.17±0.08 MPa (PLLA-CHT1) and 0.09±0.03 MPa (PLLA-CHT2), regarding pure PLLA.

3.4. Cell viability

During the follow-up period BM-MSCs cultured in the scaffolds remained metabolically active (Figure 4), showing a similar trend in their behavior, slightly decreasing their activity on day 14 and reaching a peak on cell proliferation, after 30 days. No significant differences were found amongst the 3 scaffolds neither regarding TCPS ($p > 0.05$).

3.5. BM-MSCs chondrogenic differentiation

After chondrogenic differentiation induction (30 days), histological examination of the engineered tissues in PLLA constructs revealed specific cell morphology along a vertical axis: a superficial region with flattened and elongated aligned cells; a middle and bulk region with the presence of few fibroblastic cells and a majority of rounded cells, oriented perpendicular to the surface, embedded in significant amounts of extracellular matrix (Figure 5, brackets in TB). These areas have shown to be immunopositive for zone-specific marker lubricin and for cartilage-specific markers, col-II and aggrecan, suggesting active proteoglycan synthesis and turnover and the formation of a hyaline-like tissue. In addition, PLLA revealed the highest percentage of col II-positive cells, and col-II/-I ratio, regarding CHT-coated scaffolds (Table 2).

PLLA-CHT1 synthesized a hyaline-like ECM, where most of the cells exhibited chondrocytic rounded morphology, supported by strong toluidine blue and safranin-O stainings as well as the immunolocalized col-II and aggrecan (Figure 5). Nonetheless, these findings were confined to small regions of the construct, having presented the lowest area covered by extracellular matrix (data not shown). These regions, expressed col-I and –X and were positively stained for alizarin red (Figure 5). Interestingly, at this time point, PLLA-CHT1 favored a

similar deposition of col-II in comparison to PLLA, albeit with an overall lower percentage of col-X positive cells (Table 2).

Cells in PLLA-CHT2 were morphologically comparable to the ones in PLLA and seemed to follow a similar distribution, but at the same time presented the lowest ratios for col-II/-I and -X (Table 2) and stained positive for alizarin red (Figure 5).

By day 60, cells at both PLLA and PLLA-CHT2 revealed various characteristics of a matured cartilaginous tissue, as evidenced by the presence of condensed cells in lacunae and nesting cells (Figure 5, arrows in TB). On the other hand, in PLLA-CHT1, where an early maturation had occurred by day 30, very few cells with less abundant matrix could be appreciated, associated with a weaker retention for GAGs (Figures 5, TB and SaO). Furthermore, there was a dramatic decrease of the ratios of col-II/-I or –X, which could be an indicative of matrix hypertrophy (Table 2). For the 3 scaffolds, alizarin red was found positive whilst Von Kossa staining remained negative throughout the entire experiment (Figure 5).

3.6. Gene Expression Analysis

qRT-PCR revealed differences in the relative gene expression level of the transcription factors Sox9, Runx1, aggrecan, col-II and hypertrophy-related markers, Runx2, col-I and -X, matrix-degrading enzyme metalloprotease 13 (MMP13) and osteopontin (OPN), after 30 days of chondrogenic induction (Figure 6). Sox9 expression in PLLA showed an increase of 2.0-fold over pellet culture, meanwhile in PLLA-CHT1 and –CHT2 it was slightly downregulated. A similar trend was observed for aggrecan although with a marked downregulation in both CHT-coated PLLA. At the same time we found

upregulated the expression of col-II in PLLA (4.0-fold) whilst CHT-coated scaffolds revealed a very low expression of this marker, even regarding the conventional pellet culture. Both col-I and -X expressions had an increase of 2.0-fold and 5.0-fold, respectively, regarding pellet culture; the expression was downregulated in the CHT-coated scaffolds. We couldn't find any significant difference amongst the scaffolds in the expression of Runx1 nor Runx2, although it was in all instances higher than in pellet culture. The expression of MMP13 was found higher in the 3 systems in comparison with pellet culture, with PLLA the highest upregulation (5.0-fold). Osteopontin was found downregulated.

After long-term culture (60 days), Sox9 was downregulated in all conditions, although only significant for pure PLLA. Col-II revealed a similar trend, being almost inexistent for PLLA-CHT1. On the other hand, aggrecan expression remained unchanged. Col-I and -X expression was slightly upregulated in the 3 scaffolds. Runx1 decreased in all systems, in opposite to Runx2 and MMP13 that were upregulated in CHT-coated scaffolds. In PLLA, Runx2 and MMP13 decreased whilst OPN was significantly upregulated.

4. Discussion

Biodegradable polymers as PLLA have a more than 30 years history of safe use in the medical field. Nonetheless PLLA has some inherent disadvantages for its application in tissue-engineered cartilage; its rigidity, considered appropriate for bone could limit their application for softer tissues and the lack of cell recognition sites does not favor cellular interaction. (34, 35) These could be overcome by the addition of natural hydrophilic components such as chitosan. (36)

In our study, the key to fabricate PLLA-CHT scaffolds was to choose proper solvents and controlled extraction-gelation parameters. The prepared systems presented different morphology that could at least be partially related to the methodologies used for their fabrication. (36, 37) Hence in PLLA-CHT1 (Figure 1B), a hydrogel-like coating, confined within a rather heterogeneous macroporous structure, resulted from freeze-gelation and freeze-drying processes, whilst in PLLA-CHT2 (Figure 1C), a fiber-like coating, resulted from drying the CHT solution on the surface of PLLA and neutralizing by air-drying.

The incorporation of similar contents of CHT (5-6%) (Figure 2A) led to a softening of PLLA, comprising elastic moduli values (Figure 3D) in the range of those found in the literature for human articular cartilage (0.1 to 2.5 MPa). (38) Due to its abundant number of hydrophilic groups, CHT-coating also improved PLLA hydrophilicity, observed by an increase of the water uptake ratios (Figure 2B). (9) Further, the solvents used did not dramatically alter the molecular weight and polydispersity of CHT-coated scaffolds (SO1). Thus the presence of short oligomeric chains was excluded; such chains would likely provoke acidification and compromise cell viability during cell culture. (39) In fact, no differences were found on the proliferation activity of BM-MSCs between coated and pure PLLA (Figure 4) and the cells proliferative behavior, by day 14, could be correlated to other findings on structurally similar PLLA scaffolds. (36)

Interactions between BM-MSCs and their local microenvironment are an integral part of signaling control of cell attachment, proliferation and differentiation. So, we investigated the influence of pure and CHT-coated PLLA scaffolds composition and architecture on the chondrogenic differentiation of BM-MSCs. A conventional culture system - pellet culture - was used as control,

as it provides a 3D environment with high cell density, allowing cell-cell interactions that mimic mesenchymal cell condensation, an early event of chondrogenesis during skeletal development. (31, 40)

A significant neocartilage formation was observed in pure PLLA, with a cellular organization analogous to the architecture present in normal articular cartilage (Figure 5). Interestingly, we found evidence of some differentiated cells, present in different regions of the scaffolds, which were able to produce zone-specific molecules, such as lubricin, and thus may be useful in regenerating the upper layers of articular cartilage. Robust ECM deposition during prolonged culture was supported by toluidine blue and safranin-O stainings that showed increasing metachromasia, an indicative of sulfated-GAGs deposition and accumulation in the matrix (Figure 5). In addition, higher expression of chondrogenic markers (col-II, aggrecan, Sox9 and Runx1) were obtained when compared with conventional pellet culture (Figure 6), confirmed on the protein level (S02). However the expression of hypertrophic markers (col-X, Runx2 and MMP13) overlapped with the onset of chondrogenesis, corroborated by col-X expression (Figure 6), and its high positive percentage (Table 2). Furthermore, the presence of large lacunae is a clear indicative of a switch to a hypertrophic phenotype (Figure 5, TB). This is not surprising as it known that the induction of chondrogenic differentiation of MSCs, using TGF-β3 and dexamethasone, can stimulate terminal differentiation in very early stages, entailing a developmental program as in embryonic limb development leading to transient cartilage, as found for the endochondral ossification process. (41, 42)

The introduction of chitosan is frequently referred as a positive influence in accelerating bone or cartilage tissues formation, due to the presence of

functional (hydroxyl and amino) groups. (43, 44) From our results, albeit CHT-coated scaffolds did yield significant cartilage hyaline-like ECM and increased concomitantly the ratios of col-II/-I and -X (Table 2, PLLA-CHT1, 30d and -CHT2, 60d), the expression of chondrogenesis-related markers was down-regulated. Moreover, alizarin red staining was early detected in CHT-coated scaffolds, colocalized with areas of deposition of a hyaline-like matrix (Figure 5, Alizarin red, TB and SaO). (45) Yet a higher positivity for this dye could be triggered by the ability of chitosan to adsorb to anionic dyes, such as seen for eosin. (24)

In particular, hydrogel-like coating in PLLA-CHT1, originated an unevenly cell distribution and proliferation in two distinct regions. One representing confined areas of high cellular congregation and matrix production inducing a faster development of a cartilage-like tissue (Figure 5, TB and SaO) with improved col-II/-I and -X ratios (Table 2). It is possible that this maturation could be triggered by local physiologic cues (oxygen tension, pH). (23) Other, representing areas of poor cell density and a scarcely produced matrix. In this case, CHT hydrogel-like coating could have slowed cellular infiltration resulting in decreased cell proliferation, proper cell condensation and/or *in vitro* chondrogenesis, as seen for other chitosan-coated porous scaffolds. (46, 47) Altogether, these observations suggest that cells underwent different degrees of chondrogenesis in different areas of the scaffold depending on the local composition. Early before, Ma et al., has described hydrogels with spatially heterogeneous cellular phenotypes and regional variations in ECM proteins, supporting the formation of heterogeneous structures according to different matrix components. (48) This could explain the obtained results of transcript

levels representing an average of different subpopulations and the spatial variations in local ECM protein accumulation.

In PLLA-CHT2, the cellular organization and morphology were comparable to pure PLLA. In fact, the fiber-like coating, that remained intact throughout the experiment, did not practically alter PLLA uniform macroporous structure, as can be appreciated in SEM micrographs and HE stained sections (Figures 1, A and C; and 5, dotted red circles in HE). So, in comparison to PLLA-CHT1, it seems that this fiber-like coating promotes a better chondrogenic response and at the same time may be hindering the hypertrophic process. This may be linked to a smaller available surface area that has been suggested to improve chondrogenesis by increasing the chance for cell-cell interactions as a result of decreasing the available biomaterial surface per cell. (49) The same authors compared the effect of chitosan scaffolds structure (macroporous sponges and microfibers) in the chondrogenesis of MSCs and concluded that it was superior in the microfibers, which could corroborate our findings. (50)

Furthermore, adsorption of adhesive proteins from serum such as fibronectin has shown to be highly reversible on chitosan, with most of the protein being desorbed or exchanged in the first 24h which could compromise cell adhesion and scaffold colonization by cells. (51) Other researchers have described the low capacity for cell attachment of pure chitosan materials, using chondrocytes. (34, 37) We found similar results when using BM-MSCs (data not shown).

In the future, we believe the induction of the chondrogenic differentiation of BM-MSCs on CHT-coated PLLA scaffolds can be improved by fine-tuning fabrication conditions in order to provide guidance for zonal distribution as in normal articular cartilage. (52) Moreover, further studies are required to

elucidate the dependence of the biological response on physicochemical properties of the scaffolds.

5. Conclusion

The incorporation of CHT to PLLA using different methodologies provided either hydrogel-like (PLLA-CHT1) or fiber-like (PLLA-CHT2) coatings. We found that the chondrogenic differentiation of BM-MSC was influenced by the composition and morphology of pure and CHT-coated PLLA scaffolds. Whilst a hydrogel-like coating supported the formation of heterogeneous tissues, with confined areas of matrix maturation or deficient cell condensation, a fiber-like coating induced a spatial distribution, alike pure PLLA and resembling the articular cartilage zonal distribution. Nonetheless, chondrogenic differentiation of BM-MSCs in CHT-coated scaffolds did not result in the production of a stable hyaline cartilage but rather the development into a transient endochondral cartilage.

Acknowledgements

The authors are thankful to the microscopy service of UPV for useful help and service; the Department of Orthopaedic Surgery-CHUAC for providing human samples; T. H. Gómez and M.J. Sánchez for cell isolation and SCH of INIBIC for histological processing. The *Biomedical Research Networking Center in Bioengineering, Biomaterials and Nanomedicine* (CIBER-BBN) is a national initiative of ISCIII. This study was supported by Program ACI-PROMOCIONA (ACI2010—1095), MAT2010-21611-CO3-01, Iniciativa Ingenio 2010, and Consolider Program.

References

1. Blanco, F.J., and Ruiz-Romero, C. New targets for disease modifying osteoarthritis drugs: chondrogenesis and Runx1. Ann Rheum Dis **72**, 631, 2013.

2. Johnstone, B., Alini, M., Cucchiarini, M., Dodge, G.R., Eglin, D., Guilak, F., Madry, H., Mata, A., Mauck, R.L., Semino, C.E., and Stoddart, M.J. Tissue engineering for articular cartilage repair--the state of the art. Eur Cell Mater **25**, 248, 2013.

3. Hermida-Gómez, T., Fuentes-Boquete, I., Gimeno-Longas, M.J., Muiños-López, E., Díaz-Prado, S., de Toro, F.J., and Blanco, F.J. Bone marrow cells immunomagnetically selected for CD271+ antigen promote in vitro the repair of articular cartilage defects. Tissue Eng Part A **17**, 1169, 2011.

4. Alves da Silva, M.L., Martins, A., Costa-Pinto, A.R., Correlo, V.M., Sol, P., Bhattacharya, M., Faria, S., Reis, R.L., and Neves, N.M. Chondrogenic differentiation of human bone marrow mesenchymal stem cells in chitosan-based scaffolds using a flow-perfusion bioreactor. J Tissue Eng Regen Med **5**, 722, 2011.

5. Griffon, D.J., Abulencia, J.P., Ragetly, G.R., Fredericks, L.P., and Chaieb, S. A comparative study of seeding techniques and three-dimensional matrices for mesenchymal cell attachment. J Tissue Eng Regen Med **5**, 169, 2011.

6. Fisher, O.Z., Khademhosseini, A., Langer, R., and Peppas, N.A. Bioinspired materials for controlling stem cell fate. Acc Chem Res **43**, 419, 2010.

7. Hu, J., Feng, K., Liu, X., and Ma, P.X. Chondrogenic and osteogenic differentiations of human bone marrow-derived mesenchymal stem cells on a nanofibrous scaffold with designed pore network. Biomaterials **30**, 5061, 2009.

8. Zhang, L., Hu, J., and Athanasiou, K.A. The role of tissue engineering in articular cartilage repair and regeneration. Crit Rev Biomed Eng **37**, 1, 2009.

9. Magalhães, J., Sousa, R.A., Mano, J.F., Reis, R.L., Blanco, F.J., and San Román, J. Synthesis and characterization of sensitive hydrogels based on semi-interpenetrated networks of poly[2-ethyl-(2-pyrrolidone) methacrylate] and hyaluronic acid. J Biomed Mater Res A **101**, 157, 2013.

10. Ringe, J., and Sittinger, M. Tissue engineering in the rheumatic diseases. Arthritis Res Ther **11**, 211, 2009.

11. Kretlow, J.D., and Mikos, A.G. 2007 AIChE Alpha Chi Sigma Award: From Material to Tissue: Biomaterial Development, Scaffold Fabrication, and Tissue Engineering. AIChE J **54**, 3048, 2008.

12. Nöth, U., Steinert, A.F., and Tuan, R.S. Technology insight: adult mesenchymal stem cells for osteoarthritis therapy. Nat Clin Pract Rheumatol **4**, 371, 2008.

13. Ni, P., Fu, S., Fan, M., Guo, G., Shi, S., Peng, J., Luo, F., and Qian, Z. Preparation of poly(ethylene glycol)/polylactide hybrid fibrous scaffolds for bone tissue engineering. Int J Nanomedicine **6**, 3065, 2011.

14. Deplaine, H., Ribelles, J.L.G., and Ferrer, G.G. Effect of the content of hydroxyapatite nanoparticles on the properties and bioactivity of poly(l-lactide) – Hybrid membranes. Composites Science and Technology **70**, 1805, 2010.

15. Wu, S.C., Chang, J.K., Wang, C.K., Wang, G.J., and Ho, M.L. Enhancement of chondrogenesis of human adipose derived stem cells in a hyaluronan-enriched microenvironment. Biomaterials. England 2010. pp. 631.

16. Ameer, G.A., Mahmood, T.A., and Langer, R. A biodegradable composite scaffold for cell transplantation. J Orthop Res **20**, 16, 2002.

17. Tanaka, T., Hirose, M., Kotobuki, N., Tadokoro, M., Ohgushi, H., Fukuchi, T., Sato, J., and Seto, K. Bone augmentation by bone marrow mesenchymal stem cells cultured in three-dimensional biodegradable polymer scaffolds. J Biomed Mater Res A **91**, 428, 2009.

18. Huang, Q., Goh, J.C., Hutmacher, D.W., and Lee, E.H. In vivo mesenchymal cell recruitment by a scaffold loaded with transforming growth factor beta1 and the potential for in situ chondrogenesis. Tissue Eng **8**, 469, 2002.

19. Yang, W., Gomes, R.R., Brown, A.J., Burdett, A.R., Alicknavitch, M., Farach-Carson, M.C., and Carson, D.D. Chondrogenic differentiation on perlecan domain I, collagen II, and bone morphogenetic protein-2-based matrices. Tissue Eng **12**, 2009, 2006.

20. Di Martino, A., Sittinger, M., andRisbud, M.V. Chitosan: a versatile biopolymer for orthopaedic tissue-engineering. Biomaterials **26**, 5983, 2005.

21. Zhang, Y., and Zhang, M. Synthesis and characterization of macroporous chitosan/calcium phosphate composite scaffolds for tissue engineering. J Biomed Mater Res **55**, 304, 2001.

22. Vaghani, S.S., and Patel, M.M. pH-sensitive hydrogels based on semi-interpenetrating network (semi-IPN) of chitosan and polyvinyl pyrrolidone for clarithromycin release. Drug Dev Ind Pharm **37**, 1160, 2011.

23. Vinatier, C., Mrugala, D., Jorgensen, C., Guicheux, J., and Noël, D. Cartilage engineering: a crucial combination of cells, biomaterials and biofactors. Trends Biotechnol **27**, 307, 2009.

24. Silva, J.M., Georgi, N., Costa, R., Sher, P., Reis, R.L., Van Blitterswijk, C.A., Karperien, M., and Mano, J.F. Nanostructured 3D Constructs Based on

Chitosan and Chondroitin Sulphate Multilayers for Cartilage Tissue Engineering. PLoS ONE **8**, e55451, 2013.

25. Deplaine, H., Lebourg, M., Ripalda, P., Vidaurre, A., Sanz-Ramos, P., Mora, G., Prósper, F., Ochoa, I., Doblaré, M., Gómez Ribelles, J.L., Izal-Azcárate, I., and Gallego Ferrer, G. Biomimetic hydroxyapatite coating on pore walls improves osteointegration of poly(L-lactic acid) scaffolds. J Biomed Mater Res B Appl Biomater **101**, 173, 2013.

26. Lebourg, M., Suay Antón, J., and Gomez Ribelles, J.L. Hybrid structure in PCL-HAp scaffold resulting from biomimetic apatite growth. J Mater Sci Mater Med **21**, 33, 2010.

27. He, L., Zhang, Y., Zeng, X., Quan, D., Liao, S., Zeng, Y., Lu, J., and Ramakrishna, S. Fabrication and characterization of poly(l-lactic acid) 3D nanofibrous scaffolds with controlled architecture by liquid–liquid phase separation from a ternary polymer–solvent system. Polymer **50**, 4128, 2009.

28. Ho, M.H., Kuo, P.Y., Hsieh, H.J., Hsien, T.Y., Hou, L.T., Lai, J.Y., and Wang, D.M. Preparation of porous scaffolds by using freeze-extraction and freeze-gelation methods. Biomaterials **25**, 129, 2004.

29. Brandrup, J., and Immergut, E.H. Polymer Handbook. New York: Wiley Interscience Publication, 1975.

30. Cicione, C., Díaz-Prado, S., Muiños-López, E., Hermida-Gómez, T., and Blanco, F.J. Molecular profile and cellular characterization of human bone marrow mesenchymal stem cells: donor influence on chondrogenesis. Differentiation **80**, 155, 2010.

31. Zhang, L., Su, P., Xu, C., Yang, J., Yu, W., and Huang, D. Chondrogenic differentiation of human mesenchymal stem cells: a comparison between micromass and pellet culture systems. Biotechnol Lett **32**, 1339, 2010.

32. Livak, K.J., and Schmittgen, T.D. Analysis of relative gene expression data using real-time quantitative PCR and the 2(-Delta Delta C(T)) Method. Methods **25**, 402, 2001.

33. Gibson, L.J., and Ashby, M.F. Cellular Solids: Structure and Properties. Cambridge: Cambridge University Press, 1999.

34. Fujihara, Y., Asawa, Y., Takato, T., and Hoshi, K. Tissue reactions to engineered cartilage based on poly-L-lactic acid scaffolds. Tissue Eng Part A **15**, 1565, 2009.

35. Grad, S., Zhou, L., Gogolewski, S., and Alini, M. Chondrocytes seeded onto poly (L/DL-lactide) 80%/20% porous scaffolds: a biochemical evaluation. J Biomed Mater Res A **66**, 571, 2003.

36. Izal, I., Aranda, P., Sanz-Ramos, P., Ripalda, P., Mora, G., Granero-Moltó, F., Deplaine, H., Gómez-Ribelles, J.L., Ferrer, G.G., Acosta, V., Ochoa, I., García-Aznar, J.M., Andreu, E.J., Monleón-Pradas, M., Doblaré, M., and Prósper, F. Culture of human bone marrow-derived mesenchymal stem cells on of poly(L-lactic acid) scaffolds: potential application for the tissue engineering of cartilage. Knee Surg Sports Traumatol Arthrosc **21**, 1737, 2013.

37. Correia, C.R., Moreira-Teixeira, L.S., Moroni, L., Reis, R.L., van Blitterswijk, C.A., Karperien, M., and Mano, J.F. Chitosan scaffolds containing hyaluronic acid for cartilage tissue engineering. Tissue Eng Part C Methods **17**, 717, 2011.

38. Stolz, M., Raiteri, R., Daniels, A.U., VanLandingham, M.R., Baschong, W., and Aebi, U. Dynamic elastic modulus of porcine articular cartilage determined

at two different levels of tissue organization by indentation-type atomic force microscopy. Biophys J **86**, 3269, 2004.

39. Von Recum, H.A., Cleek, R.L., Eskin, S.G., and Mikos, A.G. Degradation of polydispersed poly(L-lactic acid) to modulate lactic acid release. Biomaterials **16**, 441, 1995.

40. Yang, W., Yang, F., Wang, Y., Both, S.K., and Jansen, J.A. In vivo bone generation via the endochondral pathway on three-dimensional electrospun fibers. Acta Biomater **9**, 4505, 2013.

41. Hellingman, C.A., Koevoet, W., and van Osch, G.J. Can one generate stable hyaline cartilage from adult mesenchymal stem cells? A developmental approach. J Tissue Eng Regen Med **6**, e1, 2012.

42. Goldring, M.B., Tsuchimochi, K., and Ijiri, K. The control of chondrogenesis. J Cell Biochem **97**, 33, 2006.

43. Niu, X., Li, X., Liu, H., Zhou, G., Feng, Q., Cui, F., and Fan, Y. Homogeneous chitosan/poly(L-lactide) composite scaffolds prepared by emulsion freeze-drying. J Biomater Sci Polym Ed **23**, 391, 2012.

44. Jiao, Y., Liu, Z., and Zhou, C. Fabrication and characterization of PLLA-chitosan hybrid scaffolds with improved cell compatibility. J Biomed Mater Res A **80**, 820, 2007.

45. Abrahamsson, C.K., Yang, F., Park, H., Brunger, J.M., Valonen, P.K., Langer, R., Welter, J.F., Caplan, A.I., Guilak, F., and Freed, L.E. Chondrogenesis and mineralization during in vitro culture of human mesenchymal stem cells on three-dimensional woven scaffolds. Tissue Eng Part A **16**, 3709, 2010.

46. Casper, M.E., Fitzsimmons, J.S., Stone, J.J., Meza, A.O., Huang, Y., Ruesink, T.J., O'Driscoll, S.W., and Reinholz, G.G. Tissue engineering of cartilage using poly-epsilon-caprolactone nanofiber scaffolds seeded in vivo with periosteal cells. Osteoarthritis Cartilage **18**, 981, 2010.

47. Yang, Z., Wu, Y., Li, C., Zhang, T., Zou, Y., Hui, J.H., Ge, Z., and Lee, E.H. Improved mesenchymal stem cells attachment and in vitro cartilage tissue formation on chitosan-modified poly(L-lactide-co-epsilon-caprolactone) scaffold. Tissue Eng Part A **18**, 242, 2012.

48. Ma, K., Titan, A.L., Stafford, M., Zheng, C., and Levenston, M.E. Variations in chondrogenesis of human bone marrow-derived mesenchymal stem cells in fibrin/alginate blended hydrogels. Acta Biomater **8**, 3754, 2012.

49. Ragetly, G.R., Griffon, D.J., Lee, H.B., Fredericks, L.P., Gordon-Evans, W., and Chung, Y.S. Effect of chitosan scaffold microstructure on mesenchymal stem cell chondrogenesis. Acta Biomater **6**, 1430, 2010.

50. Ragetly, G.R., Slavik, G.J., Cunningham, B.T., Schaeffer, D.J., and Griffon, D.J. Cartilage tissue engineering on fibrous chitosan scaffolds produced by a replica molding technique. J Biomed Mater Res A **93**, 46, 2010.

51. Custódio, C.A., Alves, C.M., Reis, R.L., and Mano, J.F. Immobilization of fibronectin in chitosan substrates improves cell adhesion and proliferation. J Tissue Eng Regen Med **4**, 316, 2010.

52. Klein, T.J., Malda, J., Sah, R.L., and Hutmacher, D.W. Tissue engineering of articular cartilage with biomimetic zones. Tissue Eng Part B Rev **15**, 143, 2009.

Reprint author: Francisco J. Blanco. Servicio de Reumatología. Instituto de Investigación Biomédica de A Coruña (INIBIC). Complexo Hospitalario Universitario de A Coruña (CHUAC). Sergas. Universidade da Coruña (UDC). As Xubias, 15006. A Coruña, Spain.

Figures and Tables

Fig. 1. SEM micrographs of cross-sections of PLLA (A); CHT (B); PLLA-CHT1 (D), where CHT forms smooth pellicles, indicated by an arrow, over PLLA macroporous structure; and PLLA-CHT2 (D), where CHT forms a fibrous-like coating over PLLA micropores. Scale bars represent 500 μm.

Fig. 2. TGA thermogram of unmodified and modified PLLA (a) and the water absorption ratios (b) of PLLA, CHT, PLLA-CHT1 and –CHT2 scaffolds.

Fig. 3. Stress strain curves for PLLA, CHT, PLLA-CHT1 and –CHT2, in the dry (a) and wet (b) state. Variations on the (c) elastic modulus (E') and (d) yield strength (Ys) for PLLA, CHT, PLLA-CHT1 and –CHT2 scaffolds (n = 5). Experiments are reported for dry ( ) and wet ( ) samples.

Fig. 4. BM-MSCs viability during 30 days in PLLA, PLLA-CHT1 and -CHT2 scaffolds. Significant differences were found in different time points (*$p < 0.05$) although no difference was observed among the different scaffolds nor TCPS.

Fig. 5. Histological (HE, TB, Sa-O, Von Kossa and alizarin red) and immunolocalization (col-I, -II and -X, aggrecan and lubricin) analysis in cross-sections of PLLA, PLLA-CHT1 and –CHT2 scaffolds seeded with BM-MSCs, after 30 and 60 days, in a chondrogenic differentiation medium.

Fig. 6. Fold-change in mRNA levels of chondrogenesis and hypertrophy in BM-MSCs cultured in PLLA, PLLA-CHT1 and –CHT2 scaffolds, normalized against

expression levels of conventional pellet culture (dashed lines), after 30 and 60 days. Data represents the mean ± SD (n = 2-3). Symbols (*; † and ‡) indicate statistically significant differences ($p < 0.05$) in the expression levels at different time points and among the different scaffolds.

Table 1. List of primers used for qRT-PCR.

Table 2. Collagens (I, II and X) positivity and ratios (col-II/-I and -X) in cell-constructs, after 30 and 60 days, in chondrogenic medium. The results are represented in positive percentage regarding the total area of matrix produced.

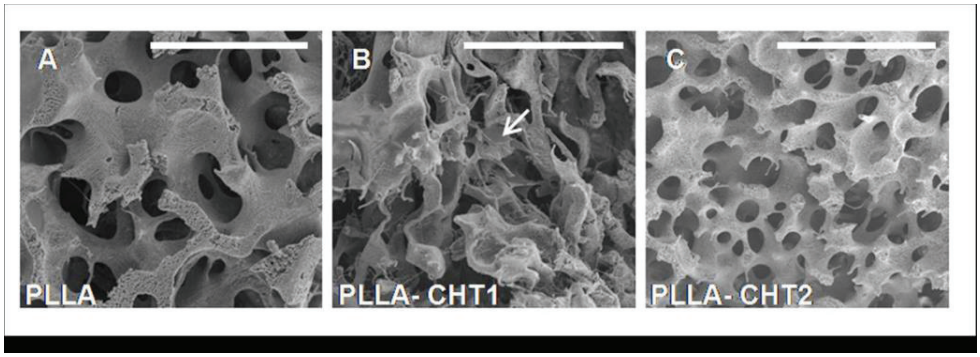

Fig. 1. SEM micrographs of cross-sections of PLLA (A); CHT (B); PLLA-CHT1 (D), where CHT forms smooth pellicles, indicated by an arrow, over PLLA macroporous structure; and PLLA-CHT2 (D), where CHT forms a fibrous-like coating over PLLA micropores. Scale bars represent 500 μm.
147x53mm (150 x 150 DPI)

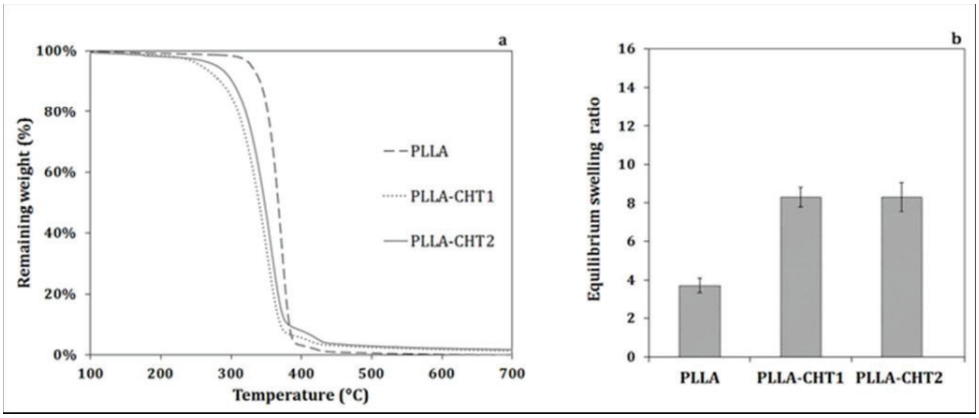

Fig. 2. TGA thermogram of unmodified and modified PLLA (a) and the water absorption ratios (b) of PLLA, CHT, PLLA-CHT1 and –CHT2 scaffolds.
215x90mm (150 x 150 DPI)

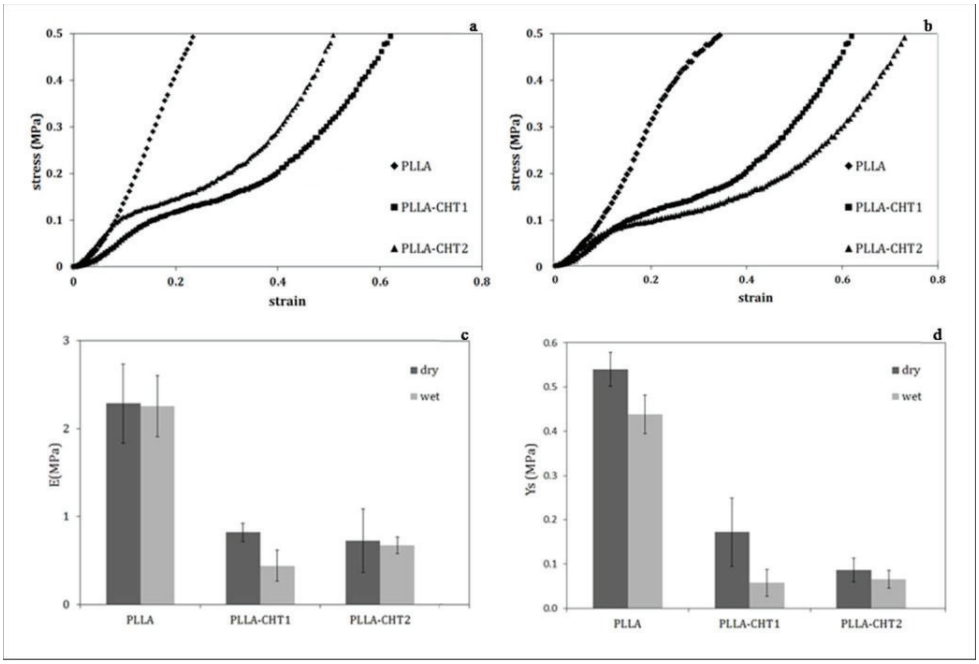

Fig. 3. Stress strain curves for PLLA, CHT, PLLA-CHT1 and –CHT2, in the dry (a) and wet (b) state. Variations on the (c) elastic modulus (E') and (d) yield strength (Ys) for PLLA, CHT, PLLA-CHT1 and –CHT2 scaffolds (n = 5). Experiments are reported for dry ( ) and wet ( ) samples.
212x143mm (150 x 150 DPI)

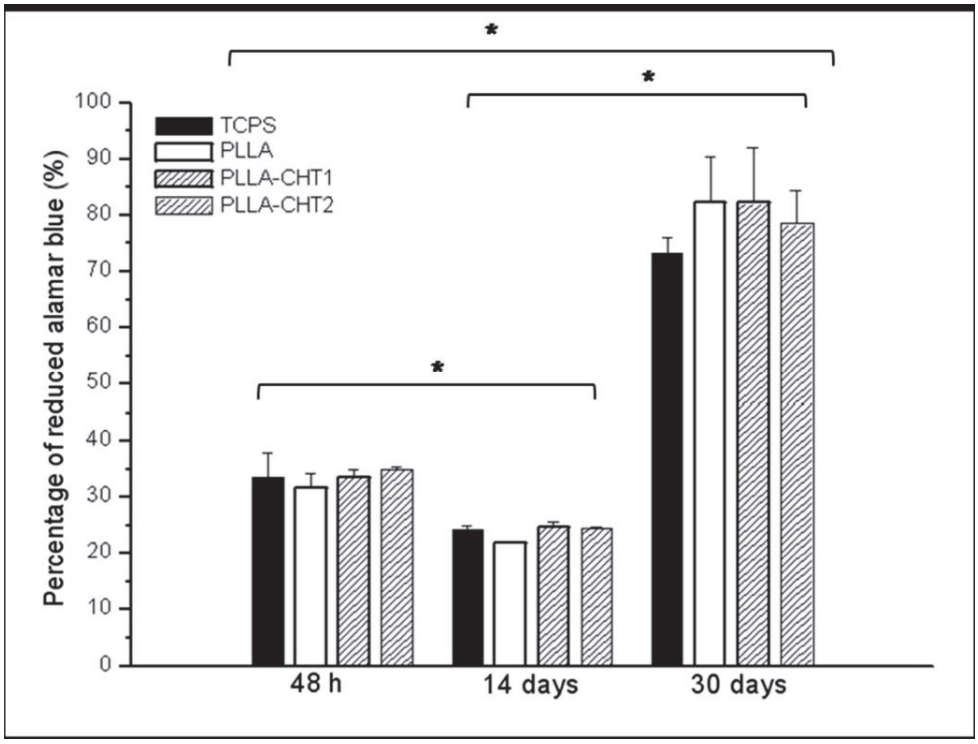

Fig. 4. BM-MSCs viability during 30 days in PLLA, PLLA-CHT1 and -CHT2 scaffolds. Significant differences were found in different time points (*p < 0.05) although no difference was observed among the different scaffolds nor TCPS.
137x103mm (150 x 150 DPI)

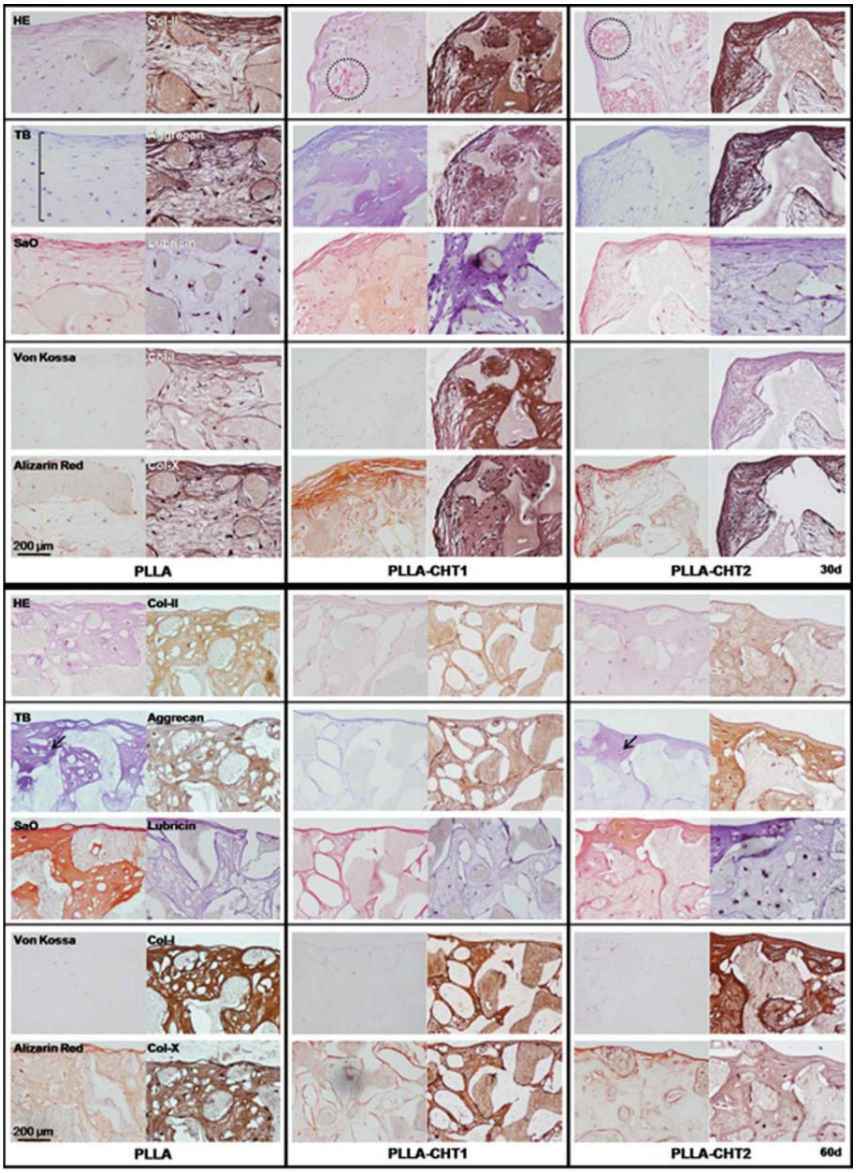

Fig. 5. Histological (HE, TB, Sa-O, Von Kossa and alizarin red) and immunolocalization (col-I, -II and -X, aggrecan and lubricin) analysis in cross-sections of PLLA, PLLA-CHT1 and –CHT2 scaffolds seeded with BM-MSCs, after 30 and 60 days, in a chondrogenic differentiation medium
100x137mm (150 x 150 DPI)

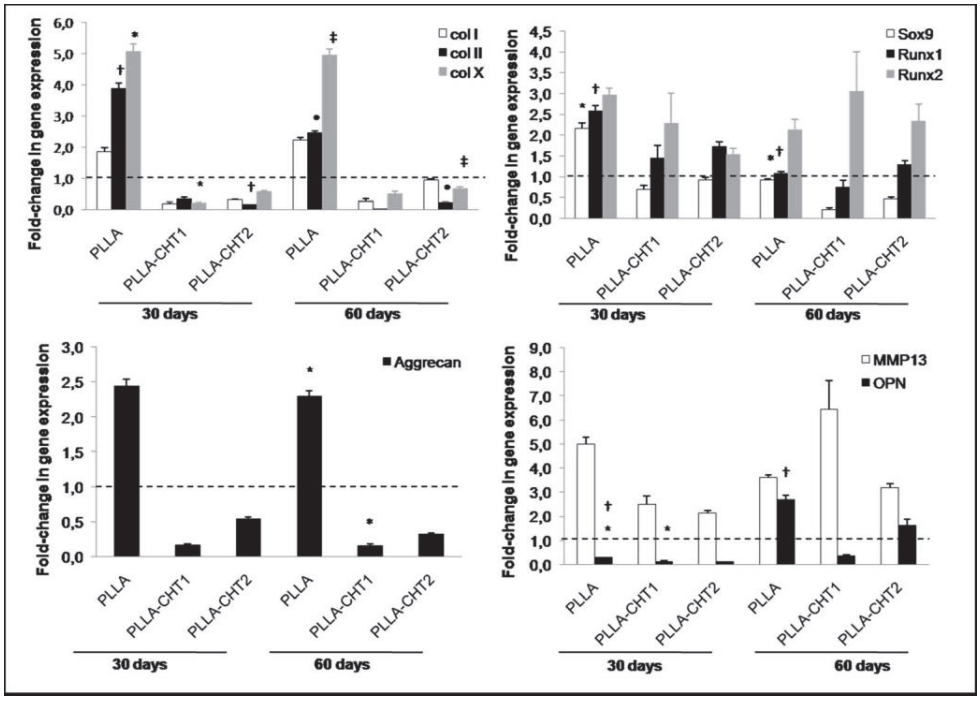

Fig. 6. Fold-change in mRNA levels of chondrogenesis and hypertrophy in BM-MSCs cultured in PLLA, PLLA-CHT1 and –CHT2 scaffolds, normalized against expression levels of conventional pellet culture (dashed lines), after 30 and 60 days. Data represents the mean ± SD (n = 2-3). Symbols (*; † and ‡) indicate statistically significant differences ($p < 0.05$) in the expression levels at different time points and among the different scaffolds.
226x161mm (150 x 150 DPI)

Table 1. List of primers used for qRT-PCR.

Gene	Forward	Reverse	Probes	Gene Bank A. Number
B2M	TTCTGGCCTGGAGGCTATC	TCAGGAAATTTGACTTTCCATTC	42	NM_004048.2
RPL13a	CAAGCGGATGAACACCAAC	TGTGGGGCAGCATACCTC	28	NM_012423.2
Sox9	GTACCCGCACTTGCACAAC	TCGCTCTCGTTCAGAAGTCTC	61	NM_000346
Aggrecan	CGGTCTACCTCTACCCTAACCA	GAGAAGGAACCGCTGAAATG	38	NM_013227.3
Col-I	CTGGCCCCATTGGTAATGT	ACCAGGGAAACCAGTAGCAC	1	NM_000088.3
Col-II	TGGTGCTAATGGCGAGAAG	CCCAGTCTCTCCACGTTCAC	4	NM_001844.4
Col-X	CACCTTCTGCACTGCTCATC	GGCAGCATATTCTCAGATGGA	6	NM_000493.3
Runx1	ACAAACCCACCGCAAGTC	CATCTAGTTTCTGCCGATGTCTT	21	NM_001122607.1
Runx2	CACCATGTCAGCAAAACTTCTT	TCACGTCGCTCATTTTGC	41	NM_001024630.3
MMP13	CCAGTCTCCGAGGAGAAACA	AAAAACAGCTCCGCATCAAC	73	NM_002427.3
OPN	CGCAGACCTGACATCCAGT	GGCTGTCCCAATCAGAAGG	61	NM_000582.2

Table 2. Collagens (I, II and X) positivity and ratios (col-II/-I and -X) in cell-constructs, after 30 and 60 days, in chondrogenic medium. The results are represented in positive percentage regarding the total area of matrix produced.

	col-I (%)	col-II (%)	col-X (%)	col-II/-I ratio	col-II/-X ratio
30 days					
PLLA	18.59	37.26	41.97	2	0.88
PLLA-CHT1	18.92	35.33	28.93	1.80	1.22
PLLA-CHT2	11.85	13.44	13.38	1.13	1.00
60 days					
PLLA	66.72	19.50	69.11	0.29	0.28
PLLA-CHT1	72.20	6.48	61.08	0.09	0.11
PLLA-CHT2	28.88	14.46	15.76	0.50	0.91

Table S01. Molecular weight of PLLA in the different samples

Sample	Mn (kDa)	Mw	Polidispersity Index
PLLA	65.6	117564	1.79
PLLA-CHT1	64.3	123233	1.91
PLLA-CHT2	61.1	121187	1.98

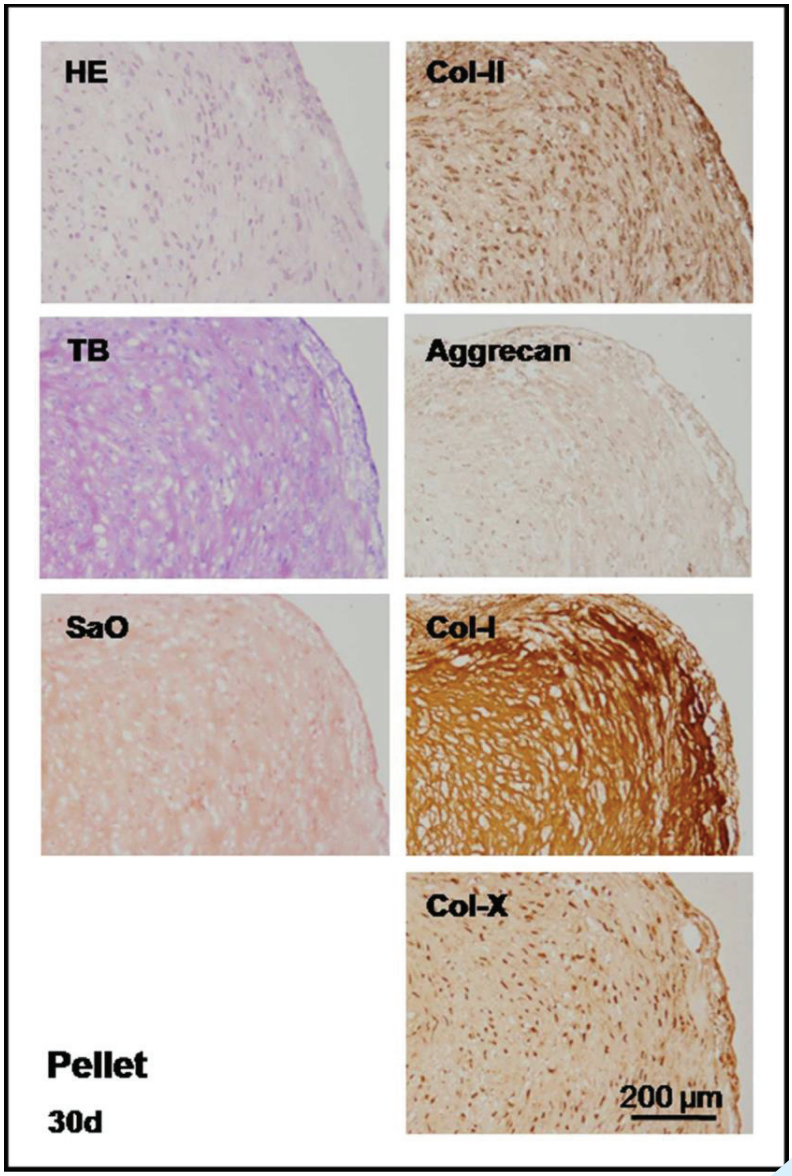

Supplementary Figure
89x133mm (150 x 150 DPI)

Supplementary Materials and Methods

Molecular weight determination

Molecular weight distribution of PLLA scaffolds pure or CHT-coated was studied by gel permeation chromatography (GPC) using a chromatograph (Waters 1525) fitted with a Binary HPLC pump (Waters 2414 Refractive Index Detector) and four serial columns (Styragel), using tetrahydrofurane (THF) as the mobile phase. Flow rate was 1.0 mL/min and the samples were prepared with 1% (w/v) in THF/Dioxane (50/50 v/v) as solvent. The concept of universal calibration was used to estimate the molecular weight of pure PLLA, using monodisperse polystyrene standards SM-105 (Showa Denko) according to the procedure reported by Painter et al. using K_{PLLA} = 5.45 x 10^5 dL/g and α_{PLLA} = 0.73, and the Mark-Houwink-Sakurada parameters for PLLA.

References

Liu, L., Fishman, M.L., Hicks, K.B., and Liu, C.K. J Agric Food Chem **53**, 9017, 2005.

Painter, P.C., and Coleman, M.M. Fundamentals of Polymer Science: An Introductory Text. Lancaster: Technomic Pub Co, 1997.